N95-10603

303168

SIMULATIONS OF ISOPRENE - OZONE REACTIONS FOR A GENERAL CIRCULATION/CHEMICAL TRANSPORT MODEL

P. A. Makar and J.C. McConnell
CRESS, York University, Toronto, Canada, M3J 1P3

Abstract:
A parameterized reaction mechanism has been created to examine the interactions between isoprene and other tropospheric gas-phase chemicals. Tests of the parameterization have shown that its results match those of a more complex reaction set to a high degree of accuracy. Comparisons between test runs have shown that the presence of isoprene at the start of a six day interval can enhance later ozone concentrations by as much as twenty-nine percent. The test cases used no input fluxes beyond the initial time, implying that a single input of a biogenic hydrocarbon to an airmass can alter its ozone chemistry over a time scale on the order of a week.

Introduction:
Various studies (cf. Jacob and Wofsy, 1988, Trainer et al., 1987) have suggested that fluxes of terpenes such as isoprene may be responsible for enhanced ozone concentrations in the lower troposphere. The full reaction mechanisms for these gases are too complex for use in chemical transport models, due to the memory space required to store all species, and the computation time needed to predict future concentrations. The present work discusses the parameterization of one of these mechanisms (that of isoprene) into a simplified form. The effect of an initial input of isoprene on later ozone chemistry was studied as part of the parameterization process.

Constructing the Parameterization.
In the following discussion, reference will be made to three reaction sets; "no isoprene", "parameterization" and "full isoprene". The first is a simplified tropospheric reaction set, following Lurmann et al. (1986) and DeMore et al (1990). The "full isoprene" set includes the no isoprene reactions and the detailed isoprene system of Lurmann et al (1986), and incorporates some of the changes suggested by Jacob and Wofsy (1988). The "parameterization" is the simplified isoprene mechanism, designed to have the same effect on the simple troposphere as the full isoprene set, yet using fewer species to accomplish this goal. The parameterized reaction mechanism and its rates are given in Appendix I.

The parameterization was constructed by eliminating unimportant reaction pathways and lumping species with similar chemistry together. In summary, the changes were:

(1) Criegee - type radicals MVKO, MAOO, and MCRG were lumped together as "CREB". The products of the oxidation of CREB by NO were determined by adding the three oxidation reactions of CREB's components.

(2) Radicals MAN_2 and MVN_2 (produced via NO_3 oxidation of methacrolein and methyl vinyl ketone, respectively) were lumped together as "MBN_2". The product coefficients for the subsequent reaction of MBN_2 with NO were derived by examining the amount of MBN_2 resulting from each of the methacrolein and methyl vinyl ketone paths.

(3) Radicals MRO_2 and VRO_2 (produced via OH reactions with MACR and MVK, respectively) were lumped together as "BRO_2", with product species and reaction coefficients adjusted as in step (2).

(4) The cycles for the natural acetyl nitrate species IPAN and MPAN were lumped together into the PAN cycle. The products leaving the cycle via oxidation of the lumped carbonate by NO are dependant on the concentrations of MACR and MVK. With this change, CH_3CHO and $HOCH_2CHO$ are lumped as a single higher aldehyde, CH_3CO_3 and MAO_3 are similarly lumped, and the total acetyl-nitrate is the sum of PAN, IPAN, and MPAN concentrations. The reaction rates used were those of the normal PAN cycle, but the products and their coefficients were changed to reflect the new sources of total PAN.

(5) Product species IPN_4, MGLO, pyruvic acid and methyl acrylic acid were dropped from the parameterization, as were the reactions for the production of ozonides.

Numerical Tests of the Parameterization:
Nine test simulations were performed, each simulation spanning six days of diurnally varying photochemistry. No fluxes or deposition were allowed after the initial start-up of the box model. The initial conditions for these tests are given in Table 1. Most of the chemicals had the same initial concentration regardless of the test. The only species with different concentrations at the initial time were NO_2, NO, O_3, PAN, and isoprene. NO_x, ozone and PAN started at three levels, representing background, rural and polluted urban air. Isoprene was set at three levels. The combinations of the three NO_x scenarios with the three isoprene levels resulted in the nine test cases. Similarly, the level of NO_x and isoprene are the only possible causes of the differences between the simulations.

Reaction rates were calculated assuming sea-level pressures at the equator close to equinox. Photochemical rates were calculated using a detailed one-dimensional model (Henderson et al., 1987). The diurnal temperature profile and an example photochemical rate are given in Figure 1.

Simulations began at noon on the first day, with the noon-to-noon diurnal profile in rates repeating during the subsequent five days.

Two types of analysis were made with the resulting data. The effect of isoprene reactions on the model atmosphere were shown by comparing no isoprene and full isoprene simulations. The parameterization results were compared to the full isoprene results in order to gauge the usefulness of the former in simulating isoprene chemistry.

Figure 1. Temperature profile and J_{NO_2}.

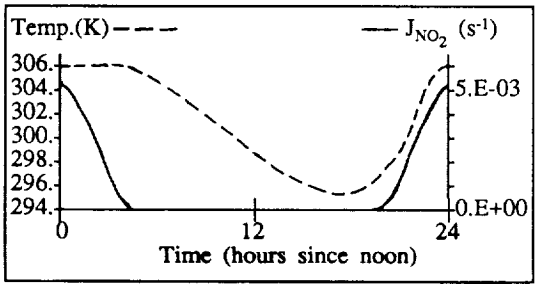

Only a few species will be shown and discussed, due to the large amount of data resulting from these simulations and the limited space for this presentation. Researchers interested in obtaining the data files or plots of the results should contact the authors at the above address.

The O_3 results for each test are given in Fig. 2. Each graph shows the concentrations (ppbv) as functions of time, and are labled according to the initial concentration scenario giving rise to the data. As can be seen from the graphs, the ozone concentration is enhanced by the addition of isoprene if the initial NO_x level is high or medium, and is depleted if the initial NO_X is low. The largest O_3 increase is for the case {high initial NO_x, high initial isoprene}, in which the ozone maximum is 25 ppbv higher after the addition of isoprene (maximum of 83.8 ppbv without isoprene, and 108.3 ppbv with initial isoprene), an enhancement of 29 % . The parameterization's O_3 values were within a few percent of those from the full isoprene mechanism for all test runs. The parameterization would appear to be suitable for O_3 simulations, with the caveat that ozone may be overpredicted by up to 5 ppbv.

The cause of the O_3 enhancements are explained via the relative steady state between O_3 and NO_X. Steady state ozone concentrations are roughly proportional to the ratio of NO_2 to NO ($O_3 \cong J_1 \bullet NO_2/(k_{14} \bullet NO)$). Reactions that bias this NO_x ratio in favour of NO_2 therefore result in higher ozone concentrations.

Two processes cause such a bias. The first is the reaction of NO with RO_2 radicals to produce NO_2. These radicals (RIO_2, INO_2, VRO_2, MVN_2, MRO_2, and MAN_2) originate from isoprene's oxidation by OH and NO_3. The reaction rates for the first hour of the "high NO_x - high Isoprene" scenario have shown that 43% of the net (positive) rate of change of NO_2 is due to production of NO_2 via the RO_2 reactions. The addition of isoprene causes the NO_2/NO ratio to move from 8.13 to 9.09.

This process is short-lived due to the rapid oxidation of isoprene and its product ketones within the first few hours of the simulation (example isoprene concentrations are given in Figure 3). This removes the source term for the RO_2 radicals. The second increase in O_3, between hours 18 and 24 (6 am and noon) is due to the release of NO_2 from the cycles of peroxyacetylnitrate (PAN) , MPAN, and

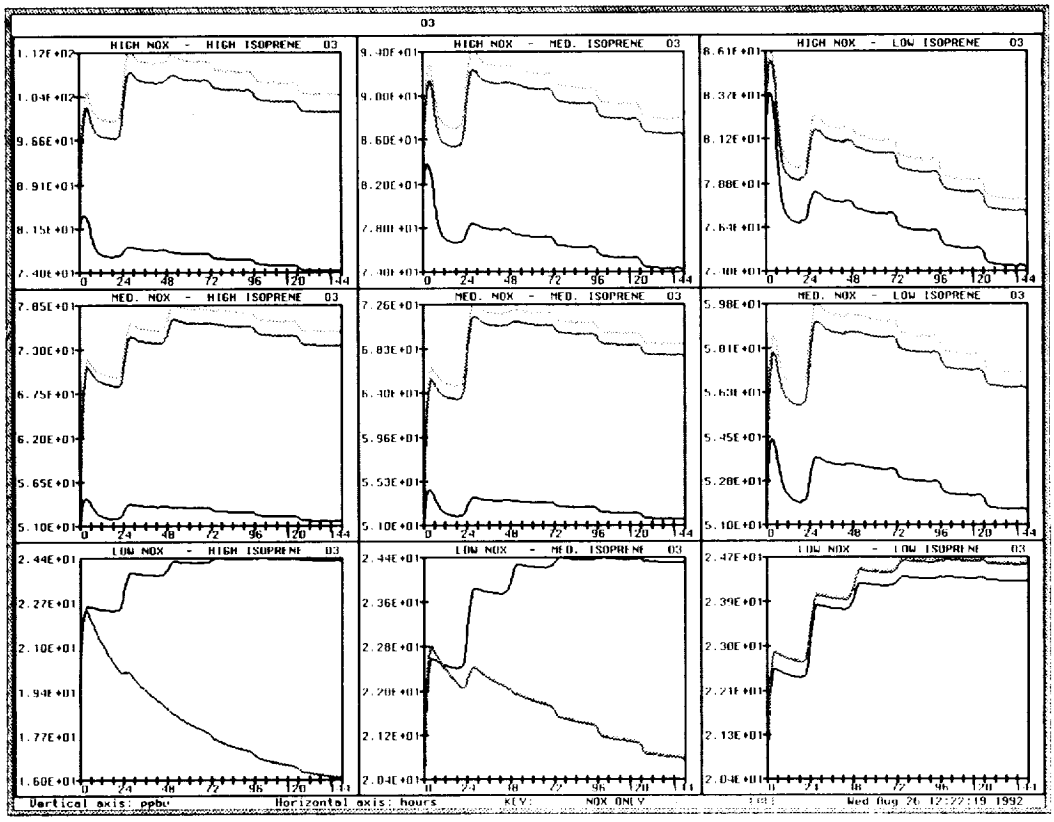

Figure 2. O_3 Concentrations, Nine test cases. Light grey, dark grey, and black lines correspond to parameterization, full isoprene, and no isoprene values, respectively.

IPAN. These species have very similar reaction chemistry (hence their combination in the parameterization); production is via reaction of a peroxyacetyl radical with NO_2, and loss is via thermal dissociation of the compound back into NO_2 and the radical. The colder temperatures during the night (hours 6 to 18) thus resulted in a buildup of the PAN-type species. The increase of temperatures on the dawn of the second day caused the release of NO_2 stored during the night as PAN, MPAN and IPAN. These processes have a magnitude sufficient to account for the entire net rate of change of NO_2 at 11:30 am on the second day.

The enhancement of O_3 due to PAN-type compounds from isoprene oxidation has important implications with regards to ozone production far from the source region. For example, NO_x produced in a region of biomass burning (a high NO_x, high isoprene source region), if carried aloft a few kilometres (a temperature contrast equivalent to the day/night one used here) could be stored as PAN and related organic compounds. Later heating of the airmass far downwind from the source would result in strongly enhanced ozone. Such a mechanism may be responsible for the "Ozone high" in the troposphere over the South Atlantic, mentioned in other papers in these Proceedings.

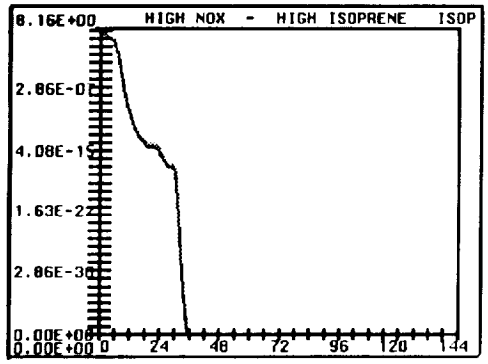

Figure 3. Isoprene Concentration, High NO_x - high isoprene. Light grey lines are parameterization results, dark grey are full isoprene mechanism.

The mechanism responsible for ozone depletion in the "low NO_x" simulations is that of removal by isoprene. Initial NO_x levels are sufficiently low so that the (RO_2 + NO) ozone source fails to compensate for the loss of ozone due to isoprene oxidation. During the first nightfall, isoprene removal of ozone dominates the other loss terms by about two orders of magnitude. Thereafter the curve describing ozone concentrations closely follows that of isoprene, with a gradual decrease in both species.

Total lumped PAN's for high NO_x - high isoprene are given in Figure 4. Total PAN has increased by about an order of magnitude for the high and medium NOx scenarios. The increase is smaller for the low NOx case, and almost non-existant for the case of low-NOx, high-isoprene. The enhancement of total PAN's is due to the addition of the biogenic MPAN and IPAN to peroxyacetylnitrate. These species increase in concentration until the middle of the second day, when the concentrations of their ketone precursors have become depleted. The enhanced PAN cycle is one of the primary causes of the ozone enhancement noted above.

Methane, ethane and propane all have a "staircase" pattern of decreasing concentration (ethane is given as an example, Figure 5). The most rapid removal (steep parts of the steps) occurs during the day, when the oxidant, OH, is highest in concentration. The differences in the rate of alkane removal between isoprene and no isoprene cases thus reflect differences in OH concentrations. Ethane removal is enhanced by the addition of isoprene in the high and medium NO_x scenarios (ie. higher OH). In the low NOx scenario, the addition of isoprene results in a decrease in the ethane removal rate (ie. lower OH). The OH values are a direct reflection of the NO_x changes discussed above. In the high NO_x - high isoprene case, daytime OH concentrations are enhanced by higher O_3 and thus higher $O(^1D)$ values. In the low NO_x - high isoprene case, daytime OH is inhibited by removal by the as yet undepleted isoprene. At hour 24 for this scenario, the loss rate of OH due to isoprene alone is 4.2 times the combined loss rates due to CO and

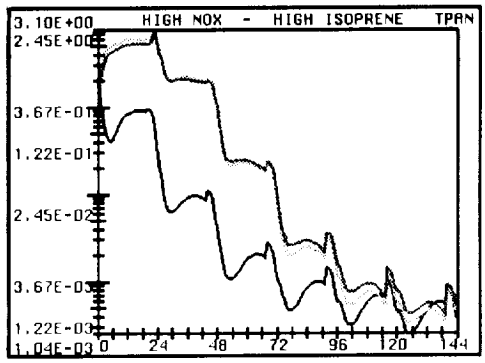

Figure 4. Total PAN (= PAN + MPAN + IPAN) Concentrations.

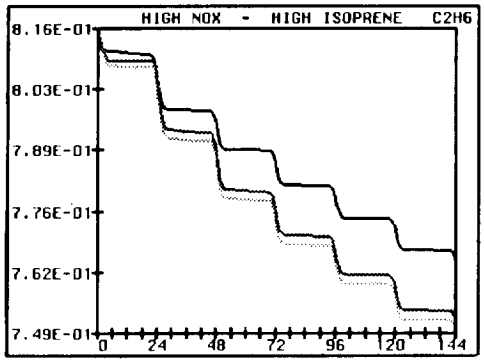

Figure 5. Ethane Concentrations.

CH_4 oxidation. When combined with the effects of its ketone products, methacrolein and methyl vinyl ketone, the isoprene-caused OH loss rate is 5.2 times the combined CO and CH_4 loss rate. In regions where the isoprene concentration is high (eg. close to the source) it will be the main chemical determining OH concentrations.

Formic acid values are given in Figure 5 (again, high NO_x - high isoprene is used as an example). The production of formic acid is greatly enhanced by the introduction of isoprene for all test cases. This is due to the addition of the creigee biradical CREA (CH_2O_2) as a source of formaldehyde.

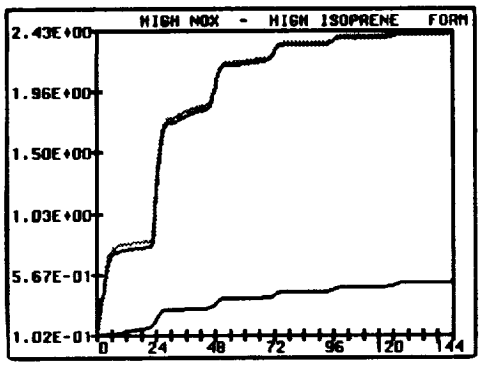

Figure 6. Formic Acid Concentrations.

Conclusions:

The isoprene parameterization derived in this work has been compared to a more detailed reaction mechanism, and has been found suitable for use in applications in which the number of chemicals are limited by computational memory and processing time. The parameterization uses 14 less species than the full mechanism, yet produces essentially the same results for the most important tropospheric gases.

The effect of isoprene on tropospheric chemistry depends on both the initial NO_x and isoprene levels. Ozone was found to either increase or decrease in concentration depending on the initial NO_X values. Increases were due to conversion of NO to NO_2, with the causes of this conversion being RO_2 reactions with NO_x and release of NO_2 from PAN -type compounds. Similar effects were shown for the other species studied. The lack of deposition or sources after the initial time showed that the injection of isoprene into an air mass can have a long term effect on the chemistry of that air mass, long after the precursor hydrocarbon has been totally oxidized.

Table 1: Initial Concentrations

Species	Concentration (ppbv)	Concentration (molecules cm^{-3})
NO_2	0.1 / 3.0 / 8.0	0.25 / 7.4 / 20.0 ($x10^{10}$)
NO	0.02 / 1.0 / 1.8	0.05 / 2.5 / 4.4 ($x10^{10}$)
O_3	20. / 50. / 80.	50. / 125. / 200. ($x10^{10}$)
NO_3	0.04 pptv	10^6
N_2O_5	0.04 pptv	10^6
PAN	0.01 / 0.3 / 8.0	0.25 / 7.5 / 20. ($x10^9$)
HNO_2	0.2	5.0 ($x10^9$)
HNO_3	2.0	5.0 ($x10^{10}$)
HNO_4	1.0 pptv	2.5($x10^7$)
CH_4	1.67 ppmv	4.185 ($x10^{13}$)
HCHO	2.0	5.0 ($x10^{10}$)
MCHO	0.5	1.25 ($x10^{10}$)
MCO_3	0.04 pptv	10^6
MOOH	0.2	5.0 ($x10^9$)
MO_2	0.04 pptv	10^6
MO	0.04 pptv	10^6
CO	200	5.0 ($x10^{12}$)
CO_2	343 ppmv	8.575 ($x10^{15}$)
C_2H_6	0.8	2.0 ($x10^{10}$)
C_3H_8	0.2	5.0 ($x10^{10}$)
ETO_2	0.04 pptv	10^6
H_2O_2	0.5	1.25 ($x10^{10}$)
HO_2	0.04 pptv	10^6
OH	0.04 pptv	10^6
FORM	0.1	2.5 ($x10^{10}$)
AHO_2	0.04 pptv	10^6
O^1D	4.0 ($x10^{-10}$)	10^1
LOSS	4.0 ($x10^{-10}$)	10^1
H_2O	1.5 %	3.829 ($x10^{17}$)
O_2		5.131 ($x10^{18}$)
M		2.45 ($x10^{19}$)

Full Isoprene Mechanism Initial Conditions:

Species	Concentration (ppbv)	Concentration (molecules cm^{-3})
ISOP	0.5 / 3.1 / 8.2	1.23 / 7.50 / 20.0 ($X10^{10}$)
MACR	0.2	5.0 ($x10^{10}$)
MVK	0.2	5.0 ($x10^{10}$)
RIO_2	0.04 pptv	10^6
INO_2	0.04 pptv	10^6
MGGY	4 pptv	10^8
IPAN	4 pptv	10^8
MPAN	4 pptv	10^8
HAC	0.01	2.5 ($x10^8$)
PYRU	0.04 pptv (all remaining species, same as PYRU)	10^6 (all remaining species; MAAC, VRO_2, MAN_2, MVN_2, MRO_2, IPN_2, CREA, MVKO, MAOO, MCRG, MGLO, HACO, MAO_3, and OZID, start at 10^6 molecules cm^{-3}).

Parameterization:
ISOP, MACR, MVK, RIO_2, INO_2, MGGY, CREA are same as above. The radicals CREB, MBN_2, and BRO_2 all start at 10^6 molecules cm^{-3}. The lumped PAN has initial concentrations of $4.5x10^8$, $7.7x10^8$, and $2.02x10^9$ molecules cm^{-3}, for low, medium and high NO_x scenarios. The lumped MCHO concentration is $1.275x10^{10}$ molecules cm^{-3}.

Appendix I : Reaction Mechanisms

No	Isoprene Reaction Mechanism	k_a	k_b	TYPE	SOURCE
1	$NO_2 + h\nu \rightarrow NO + O_3$			1	a
2	$O_3 + h\nu \rightarrow O(^1D) + O_2$			1	a
3	$H_2O_2 + h\nu \rightarrow 2\ OH$			1	a
4	$HCHO + h\nu \rightarrow H_2 + CO$			1	a
5	$HCHO + h\nu \rightarrow 2\ HO_2 + CO$			1	a
6	$MOOH + h\nu \rightarrow MO + OH$			1	a
7	$N_2O_5 + h\nu \rightarrow NO_2 + NO_3$			1	a
8	$HNO_3 + h\nu \rightarrow OH + NO_2$			1	a
9	$MCHO + h\nu \rightarrow MO_2 + HO_2 + CO$			1	a
10	$NO_3 + h\nu \rightarrow NO + O_2$			1	a
11	$NO_3 + h\nu \rightarrow NO_2 + O_3$			1	a
12	$O(^1D) + M \rightarrow O_3 + M$	special function		4	a
13	$O(^1D) + H_2O \rightarrow 2\ OH$	2.2E-10		3	a
14	$O_3 + NO \rightarrow NO_2 + O_2$	2.0E-12	1.4E+03	2	a
15	$O_3 + OH \rightarrow HO_2 + O_2$	1.6E-12	9.4E+02	2	a
16	$O_3 + HO_2 \rightarrow OH + 2\ O_2$	1.1E-14	5.0E+02	2	a
17	$O_3 + NO_2 \rightarrow NO_3 + O_2$	1.2E-13	2.45E+03	2	a
18	$OH + H_2O_2 \rightarrow HO_2 + H_2O$	2.9E-12	1.6E+02	2	a
19	$OH + NO \rightarrow HNO_2$	special function		4	b
20	$OH + NO_2 \rightarrow HNO_3$	special function		4	a
21	$OH + HNO_3 \rightarrow NO_3 + H_2O$	special function		4	a
22	$OH + CO \rightarrow HO_2 + CO_2$	special function		4	a
23	$OH + CH_4 \rightarrow MO_2 + H_2O$	2.3E-12	1.7E+03	2	a
24	$OH + HCHO \rightarrow HO_2 + CO + H_2O$	1.0E-11		3	a
25	$OH + MOOH \rightarrow MO_2 + H_2O$	3.8E-12	-2.0E+02	2	a
26	$OH + MCHO \rightarrow MCO_3 + H_2O$	6.9E-12	-2.5E+02	2	b
27	$HO_2 + NO \rightarrow NO_2 + OH$	3.7E-12	-2.4E+02	2	a
28	$HO_2 + OH \rightarrow H_2O + O_2$	4.8E-11	-2.5E+02	2	a
29	$2\ HO_2 \rightarrow H_2O_2 + O_2$	2.3E-13	-6.0E+02	2	a
30	$HO_2 + MO_2 \rightarrow MOOH + O_2$	3.3E-13	-8.0E+02	2	a
31	$HO_2 + MCO_3 \rightarrow$ LOSS	3.0E-12		3	b
32	$HO_2 + NO_2 \rightarrow HNO_4$	special function		4	b
33	$NO_2 + NO_3 \rightarrow N_2O_5$	special function		4	a
34	$NO_2 + NO_3 \rightarrow NO + NO_2 + O_2$	2.5E-14	1.23E+03	2	b
35	$N_2O_5 \rightarrow NO_2 + NO_3$	special function		4	b
36	$NO_3 + NO \rightarrow 2\ NO_2$	8.0E-12	-2.5E+02	2	b
37	$NO_3 + HCHO \rightarrow HNO_3 + HO_2 + CO$	3.2E-16		3	b
38	$NO + MO_2 \rightarrow NO_2 + MO$	4.2E-12	-1.8E+02	2	b
39	$NO_2 + MCO_3 \rightarrow PAN$	4.7E-12		3	b
40	$NO + MCO_3 \rightarrow MO_2 + CO_2 + NO_2$	4.2E-12	-1.8E+02	2	b
41	$PAN \rightarrow MCO_3 + NO_2$	1.95E+16	9.0E+02	2	a
42	$MO + O_2 \rightarrow HCHO + HO_2$	3.94E-14	9.0E+02	2	a
43	$N_2O_5 + H_2O \rightarrow 2\ HNO_3$	1.3E-21		3	b
44	$C_2H_4 + OH \rightarrow ETO_2 + H_2O$	1.7E-11	1.232E+03	2	b
45	$ETO_2 + NO \rightarrow MCHO + HO_2 + NO_2$	4.2E-12	-1.8E+02	2	b
46	$2\ ETO_2 \rightarrow 1.6\ MCHO + 1.2\ HO_2$	5.0E-14		3	b
47	$ETO_2 + HO_2 \rightarrow$ LOSS	3.0E-12		3	b
48	$C_3H_8 + OH \rightarrow ETO_2$	1.18E-11	6.79E+02	2	b
49	$MCHO + NO_3 \rightarrow MCO_3 + HNO_3$	1.4E-12	1.9E+03	2	a
50	$HNO_4 \rightarrow NO_2 + HO_2$	special	function	4	b
51	$HNO_2 + h\nu \rightarrow NO + OH$	0.205 x	$J(NO_2)$	1	b
52	$HCHO + HO_2 \rightarrow AHO_2$	1.0E-14		3	b
53	$AHO_2 + NO \rightarrow FORM + HO_2 + NO_2$	4.2E-12	-1.8E+02	2	b
54	$AHO_2 + HO_2 \rightarrow FORM + H_2O + O_2$	2.0E-12		3	b
55	$2\ AHO_2 \rightarrow 2\ FORM + 2\ HO_2 + 2\ O_2$	1.0E-13		3	b
56	$FORM + OH \rightarrow HO_2 + H_2O + CO_2$	3.2E-13		3	b

Comments:
(1) Photolysis rates from detailed model results at 0 km (see text).
(2) Temperature dependant rates, $k = k_a \times \exp(-k_b/T)$, T =temp. in K.
(3) Constant rates.

C-2

(4) Special functions for given reactions:

(12) The reaction $O(^1D) + M \rightarrow O_3 + M$ (the products are actually $O(^3P) + M$, but the conversion to O_3 is assumed to be "instantaneous") is a combination of the reactions

$O(^1D) + N_2 \rightarrow O(^3P) + N_2$, $k=1.8E\text{-}11 \bullet e^{110/T}$, and

$O(^1D) + O_2 \rightarrow O(^3P) + O_2$, $k=3.2E\text{-}11 \bullet e^{70/T}$.

If 80 % of M is N_2, and 20 % is O_2, then the net reaction is

$O(^1D) + M \rightarrow O_3 + M$, and

$k_{net} = 1.44E\text{-}11 \bullet e^{110/T} + 6.4E\text{-}12 \bullet e^{70/T}$

(19) $$k = \left(\frac{A \bullet T^B \bullet [M]}{1 + \frac{A \bullet T^B \bullet [M]}{C \bullet T^D}}\right) \bullet 0.6^{\left(1 + \left(\log_{10}\frac{A \bullet T^B \bullet [M]}{C \bullet T^D}\right)^2\right)^{-1}}$$

A = 1.0E-22, B = -3.3, C = 9.0E-09, D = -1.0

(20) $$k = \left(\frac{A \bullet [M]}{1 + \frac{A \bullet [M]}{B}}\right) \bullet 0.6^{\left(1 + (\log_{10}\frac{A \bullet [M]}{B})^2\right)^{-1}}$$

$A = 2.6E\text{-}30 \bullet (T/300)^{-3.2}$, $B = 2.4E\text{-}11 \bullet (T/300)^{-1.3}$

(21) $$k = A + \frac{C \bullet [M]}{1 + \frac{C \bullet [M]}{B}}$$, $A = 7.2E\text{-}15 \bullet \exp(785 / T)$,

$B = 4.1E\text{-}16 \bullet \exp(1440/T)$, $C = 1.9E\text{-}33 \bullet \exp(725 / T)$.

(22) $k = 1.50E\text{-}13 \bullet (1 + 0.6 \bullet [M] \bullet T \bullet 1.36E\text{-}16 / 1.013E+06)$

(32) $$k = \left(\frac{6.9E\text{-}33 \bullet [M] \bullet e^{1007/T}}{1 + 4.86E\text{-}12 \bullet [M]^{0.87}}\right)$$

(33) (same formula as reaction 20),

$A = 2.2E\text{-}30 \bullet (T/300)^{-4.3}$, $B = 1.5E\text{-}12 \bullet (T/300)^{-0.5}$

(35) $k = k_{33} \bullet 7.5E+26 \bullet (300/T)^{0.32} \bullet e^{-11080/T}$

(50) $k = (4.9E\text{-}06 \bullet [M] \bullet \exp(-10015/T)) / (1 + 4.86E\text{-}12 \bullet [M]^{0.61})$

In the above, [M] is the total number density in molecules cm^{-3}, and T is the temperature in degrees Kelvin.

Sources: (a) DeMore et al, 1990, (b) Lurmann et al., 1986

Parameterization Reactions:

57	ISOP + O_3	→ 0.5 HCHO	+ 0.2 MVK	+ 0.30 MACR + 0.2 CREA	+ 0.06 HO_2	+ 0.5 CREB	7.0E-15 1.9E+03 2
58	MVK + O_3	→ 0.5 HCHO	+ 0.2 CREA	+ 0.21 HO_2 + 0.2 CREB	+ 0.15 MCHO	+ 0.5 MGGY + 0.15 MCO_3	4.0E-15 2.0E+03 2
59	MACR + O_3	→ 0.5 HCHO	+ 0.2 CREA	+ 0.21 HO_2 + 0.15 MO_2	+ 0.5 MGGY		4.4E-15 2.5E+03 2
60	ISOP + OH	→ RIO_2					1.5E-11 -5.0E+02 2
61	RIO_2 + NO	→ 0.9 NO_2	+ 0.45 MVK	+ 0.45 MACR + 0.9 HO_2	+ 0.9 HCHO		4.2E-12 -1.8E+02 2
62	INO_2 + NO	→ 2.0 NO_2	+ HCHO	+ 0.5 MVK + 0.5 MACR			4.2E-12 -1.8E+02 2
63	INO_2 + NO_2	→ LOSS					4.2E-13 -1.8E+02 2
64	ISOP + NO_3	→ INO_2					3.23E-13 3
65	CREA + H_2O	→ FORM	+ H_2O				4.0E-18 3
66	CREA + NO	→ HCHO	+ NO_2				7.0E-12 3
67	CREA + NO_2	→ HCHO	+ NO_3				7.0E-13 3
68	CREB + H_2O	→ LOSS	+ H_2O				4.0E-18 3
69	CREB + NO	→ 0.33 MVK	+ 0.33 MACR	+ 0.33 MGGY + NO_2			4.2E-12 -1.8E+02 2
70	CREB + NO_2	→ 0.33 MVK	+ 0.33 MACR	+ 0.33 MGGY + NO_3			4.2E-13 -1.8E+02 2
71	RIO_2 + HO_2	→ LOSS					3.0E-12 3
72	INO_2 + HO_2	→ LOSS					3.0E-12 3
73	MACR + NO_3	→ MBN_2					6.7E-15 3
74	MVK + NO_3	→ MBN_2					6.0E-14 3
75	MBN_2 + NO	→ 2.0 NO_2	+ HCHO	+ 0.45 HO_2 + 0.45 MCO_3	+ 0.55 MGGY		4.2E-12 -1.8E+02 2
76	MACR + NO_3	→ MCO_3	+ HNO_3				3.3E-15 3
77	MGGY	→ MCO_3	+ HO_2				0.15 ×J(NO_2)
78	MGGY + OH	→ MCO_3					1.7E-11 3
79	MACR + OH	→ BRO_2					3.86E-12 -5.0E+02 2
80	MACR + OH	→ MCO_3					1.02E-11
81	MVK + OH	→ BRO_2					3.0E-12 -5.0E+02 2
82	BRO_2 + HO_2	→ LOSS					3.0E-12 3
83	BRO_2 + NO	→ 0.9 NO_2	+ 0.625 HO_2	+ 0.625 HCHO + 0.625 MGGY	+ 0.275 MCO_3	+ 0.275 MCHO	4.2E-12 -1.8E+02 2
84	MBN_2 + HO_2	→ LOSS					3.0E-12 3

Comments:

(1) The first 56 reactions are those of the "No Isoprene" set, with the exception of reaction 40, which has been altered to reflect the lumped PAN cycle. Reaction 40 is replaced with:

$$MCO_3 + NO \rightarrow a\ MO_2 + a\ CO_2 + (a+3b)\ NO_2 + b\ HO_2 + b\ MGGY - 2b\ NO,$$

$$b = \frac{k_{7,6}(MACR)(NO_3) + k_{8,6}(MACR)(OH)}{\left[(k_{1,6}(NO_3)+k_{8,6}(OH))(MACR) + (k_{4,6}(NO_3)+k_{14}(OH))(MCHO) + 0.15\ k_{7,8}(MVK)(O_3) + (0.45\ k_{7,5}(MBN_2) + 0.275\ k_{8,1}(BRO_2))(NO) + (k_{7,7} + k_{7,8}(OH))(MGGY)\right]}$$

and $a = 1.0 - b$. In the parameterization, "MCO_3", "MCHO", and "PAN" refer to the lumped peroxyacetyl radical, lumped higher aldehyde and lumped acetylnitrate species, respectively.

(2) Temperature dependant rates: $k=k_o \exp(-k_r/T)$, T = temperature in degrees K.

(3) Constant rates.

REFERENCES

DeMore, W.B., S.P. Sander, D.M. Golden, M.J. Molina, R.F. Hampson, M.J. Kurylo, C.J. Howard, A.R. Ravishankara, 1990: Chemical Kinetics and Photochemical Data for Use in Stratospheric Modelling. J.P.L. Publication 90-1, 1990, Jet Propulsion Laboratories, California Institute of Technology, Pasadena, California.

Henderson, G.S, W.F.J. Evans, J.C. McConnell and E.M.J. Templeton, 1987: A Numerical Model for One Dimensional Simulation of Stratospheric Chemistry. Atmosphere - Ocean, 25, 427 - 459.

Jacob, D.J., and S.C. Wofsy, 1988: Photochemistry of Biogenic Emissions Over the Amazon Forest. J. Geophys. Res., 93, **D4**, 1,477 - 1,486.

Lurmann, F.W., A.C. Lloyd, and R. Atkinson, 1986: A Chemical Mechanism for Use in Long-Range Transport/Acid Deposition Computer Modeling. J. Geophys. Res., 91, **D10**, 10,905 - 10,936.

Trainer, M., E.Y. Hsie, S.A. McKeen, R. Tallamraju, D.D. Parrish, F.C. Fehsenfeld, and S.C. Liu, 1987: Impact of Natural Hydrocarbons on Hydroxyl and Peroxy Radicals at a Remote Site. J. Geophys. Res., 92, **D10**, 11,879 - 11,894.